The generalized cross validation method for the selection of regularization parameter in geophysical diffraction tomography

E. T. F. Santos*

CEFET/BA, Salvador, Brazil and Stanford University

A. Bassrei†

Institute of Physics & Research Center in Geophysics and Geology, Federal University of Bahia, Salvador, Brazil

J. Harris‡

Departament of Geophysics, Stanford University

(Dated: July 20, 2007)

Inverse problems are usually ill-posed in such a way that it is necessary to use some method to reduce their deficiencies. The method that we choose is the regularization by derivative matrices. There is a crucial problem in regularization, which is the selection of the regularization parameter λ. In this work we use generalized cross validation (GCV) as a tool for the selection of λ. GCV was presented by Golub et al. (1979), and it is used in this work in geophysical diffraction tomography, where the objective is to obtain the 2–D velocity distribution from the measured values of the scattered acoustic field. The results are compared to those obtained using L-curve, and also Θ-curve, which is an extension of L-curve (Santos and Bassrei, 2007). We present several simulation results with synthetic data, and in general, the results using GCV are better that the other two approaches.

PACS numbers: 43.20.El, 43.20.Fn, 43.40.Le, 43.40.Ph, 43.60.Pt, 43.60.Rw

I INTRODUCTION

The main purpose of exploration geophysics for hydrocarbons is to provide trustworthy images of the subsurface, which could indicate potential hydrocarbon reservoirs. Exploration seismology, better known as seismics, is the area of applied geophysics most employed for the subsurface imaging in hydrocarbons reservoirs. And within seismics, tomography was incorporated as a suitable method of data inversion. In this work we use geophysical diffraction tomography where the input data is the scattered acoustic field measured at the receivers, and the velocity of the 2–D medium is the inversion output. Instead of using the classical approach of diffraction tomography in geophysics, that is, Fourier projection theorem (Devaney, 1984; Slaney at al., 1984; Wu and Toksöz, 1987), we use a matrix formulation approach (Thompson et al., 1994; Reiter and Rodi, 1996; Rocha Filho et al., 1996, 1997). The main advantages of the matrix formulation are: (1) the option of having irregular spacing (i) between sources, (ii) between receivers and (iii) between sources and receivers (all very common in practical situations with real data); and (2) the possibility to study, in a better way, the ill-posedness of the inverse problem. The main disadvantage is the cost in terms of computation time. For the forward modeling we compute the scattered acoustic field from a given 2–D velocity distribution. The field is obtained by a second order in time and fourth order in space finite difference scheme, and the tomographic matrix by a first order Born approximation. One common way to calculate inverse matrix is by the generalized inverse through singular value decomposition.

Since geophysical diffraction tomography is an ill-posed inverse problem, it is necessary to use some tool to reduce this deficiency. The tool that we choose is the regularization of the inverse problem by derivative matrices, known in the literature by several names, specially as Tikhonov regularization. Regularization has an input parameter with crucial role, known as regularization parameter λ, which choice is already a problem.

Yao and Roberts (1999), presented an algorithm for the practical choice of the regularization parameter in linear seismic tomographic inversion. Two criteria for the choice of the regularization parameter were investigated. The first approach assumes that norm of the errors in observed data is known accurately and searches the regularization parameter associated with this error using Newton's method. The second approach is the application of generalized cross-validation (GCV), which chooses the regularization parameter associated with the best average prediction for all possible omissions of one datum, corresponding to the minimizer of GCV function. More recently, Farquharson and Oldenburg (2004) compared two automatic ways of estimating the best regular-

*Electronic address: etfs@cpgg.ufba.br
†Electronic address: bassrei@cpgg.ufba.br
‡Electronic address: harris@pangea.stanford.edu

ization parameter to non-linear inverse problems: GCV and L-curve. These criteria initially proposed for linear problems are applied to each iteration of linearized inverse problems, in a typical iterative process to obtain the linearized solution to the corresponding non-linear problem. Thus, the best λ is estimated for each linearized iteration. To ensure that the regularization parameter decreases along iterations, an attenuation factor is multiplied by the regularization parameter at last iteration to limit the next maximum allowable parameter.

In the present work, to our knowledge the first one in geophysical diffraction tomography using regularization with search for the optimum parameter, we employ GCV in cross-hole and vertical seismic profile (VSP) geophysical diffraction tomography. We compare the GCV results with two other approaches: L-curve and Θ-curve.

II LINEAR INVERSION TECHNIQUES

Consider a modeling process where the input of some system is described by certain parameters contained in $\mathbf{m}$ and the output is described as $A\mathbf{m}(=\mathbf{d})$ which is a linear transformation on $\mathbf{m}$. If the vector $\mathbf{d}$ describes the observed output of the system, the problem is to "choose" the parameters $\mathbf{m}$ in order to minimize in some sense, the difference between the observed $\mathbf{d}$ and the prescribed output of the system $A\mathbf{m}$. If we measure this difference through the norm $\| \bullet \|$, our task is to find the value of $\mathbf{m}$ which minimizes

$$\| A\mathbf{m} - \mathbf{d} \|_2, \tag{1}$$

where the $M \times N$ matrix A and the data vector $\mathbf{d}$ with M elements are provided to the problem. This is called a least squares problem, which can formally stated as follows. Considering the basic relationship

$$\mathbf{d} = A\mathbf{m}, \tag{2}$$

we wish to minimize the error using the following objective function:

$$\Phi(\mathbf{m}) = \mathbf{e}^T \cdot \mathbf{e} + \lambda L_2, \tag{3}$$

where the error is given by $\mathbf{e} = \mathbf{d} - A\mathbf{m}$, λ is a scalar called the damping parameter and $L_2 = \mathbf{m}^T \cdot \mathbf{m}$. The estimated solution, also called damped least squares (DLS) solution, is

$$\mathbf{m}^{est} = (A^T A + \lambda I)^{-1} A^T \mathbf{d}. \tag{4}$$

The generalized inverse is frequently used in the inversion of geophysical data and its respective solution has the minimum norm. In this case the objective function to be minimized is

$$\Phi(\mathbf{m}) = \mathbf{m}^T \cdot \mathbf{m} + \mathbf{t}^T \cdot (\mathbf{d} - A\mathbf{m}), \tag{5}$$

where $\mathbf{t}$ is the vector of Lagrange multipliers. The minimization yields

$$\mathbf{m}^{est} = A^T (AA^T)^{-1} \mathbf{d}. \tag{6}$$

Consider a $M \times N$ matrix A. If: (i) $AA^+A = A$, (ii) $A^+AA^+ = A^+$, (iii) $(AA^+)^T = AA^+$, and (iv) $(A^+A)^T = A^+A$, then the $N \times M$ matrix A^+ is unique. The GI is usually calculated using the singular value decomposition (SVD). A rectangular $M \times N$ matrix A with rank k can be decomposed as $A = U\Sigma V^T$, where U is the $M \times M$ matrix which contains the orthonormalized eigenvectors of AA^T, V is the $N \times N$ matrix which contains the orthonormalized eigenvectors of A^TA and Σ is the $M \times N$ diagonal matrix which contains the singular values of A, written in the decreasing order, that is, $\sigma_1 \geq \sigma_2 \geq ... \geq \sigma_k$. The GI A^+ is a $N \times M$ matrix given by $A^+ = V\Sigma^+U^T$, where Σ^+ is the $N \times M$ diagonal matrix which contains the reciprocals of the non-zero singular values of A, so that

$$\Sigma^+ = \begin{pmatrix} E & 0 & \cdots & 0 \\ 0 & 0 & \cdots & 0 \\ \vdots & \vdots & \ddots & \vdots \\ 0 & 0 & \cdots & 0 \end{pmatrix}, \tag{7}$$

and E is the diagonal square matrix of order k expressed by

$$E = \begin{pmatrix} \sigma_1^{-1} & 0 & \cdots & 0 \\ 0 & \sigma_2^{-1} & \cdots & 0 \\ \vdots & \vdots & \ddots & \vdots \\ 0 & 0 & \cdots & \sigma_k^{-1} \end{pmatrix}. \tag{8}$$

III REGULARIZATION AND GENERALIZED CROSS VALIDATION

Least-squares solutions very often do not provide good results and sometimes they do not even exist. In order to solve this problem we use a tool of regularization or smoothing: the ill-conditioning of the matrix A is regularized and the unstable least-squares estimate $\mathbf{m}^{est}$ is consequently smoothed to greatly reduce the possibility of wild noise-induced fluctuation in $\mathbf{d}$, hopefully without distorting the resulting smoothed image too far from the true $\mathbf{m}$ (Titterington, 1985).

The concept of regularization was introduced by Tikhonov in 1963 in order to improve the quality of the inversion. This theory was studied by many researchers, and we use the Twomey (1963) approach. See Bassrei and Rodi (1993) for a little bit more about names and history in regularization theory. Consider the following objective function:

$$\Phi(\mathbf{m}) = \lambda (D_l \mathbf{m})^T D_l \mathbf{m} + \mathbf{e}^T \mathbf{e}, \tag{9}$$

where λ is the regularization parameter and D_l is the l^{th}-order derivative matrix. If $\partial\Phi(\mathbf{m})/\partial\mathbf{m} = 0$, then the estimated model is given by

$$\mathbf{m}^{est} = (A^T A + \lambda D_l^T D_l)^+ A^T \mathbf{d}. \tag{10}$$

Notice that if $\lambda = 0$ we obtain the standard least squares, and the least squares is said to be damped if $D_0^T D_0 = I$.

If D is the first derivative matrix then the regularization is called to be first order and so on. Each 2D model was scanned line by line to be represented by a single vector, that is, rasterized. It simplifies the form of the discrete derivative approximation matrix, which resembles a regular pattern. Thus, the matrices D_1 and D_2 may be schematized by the following templates:

$$D_1 = \begin{pmatrix} -1 & 1 & 0 & 0 & 0 & 0 & 0 & \cdots & 0 \\ 0 & -1 & 1 & 0 & 0 & 0 & 0 & \cdots & 0 \\ \vdots & & & \vdots & \ddots & \vdots & & & \ldots \\ 0 & \cdots & 0 & 0 & 0 & 0 & -1 & 1 & 0 \\ 0 & \cdots & 0 & 0 & 0 & 0 & 0 & -1 & 1 \end{pmatrix}, \qquad (11)$$

and

$$D_2 = \begin{pmatrix} 1 & -2 & 1 & 0 & 0 & 0 & 0 & \cdots & 0 \\ 0 & 1 & -2 & 1 & 0 & 0 & 0 & \cdots & 0 \\ \vdots & & & & \ddots & & & & \ldots \\ 0 & \cdots & 0 & 0 & 0 & 1 & -2 & 1 & 0 \\ 0 & \cdots & 0 & 0 & 0 & 0 & 1 & -2 & 1 \end{pmatrix}. \qquad (12)$$

For the determination of the optimum parameter we used the GCV (generalized cross validation) approach. GCV is based on the principle of cross validation, that is, the regularized inverse problem is solved omitting at each realization one point of the observed data. For each realization is used a given regularization parameter λ. It is expected that the adopted λ is adequate, that is, the estimated data parameters obtained by forward modeling for the for the k-th iteration ($\mathbf{d}_k^{calc}(\mathbf{m}_k^{est})$) is near to the observed data parameters. Thus the optimum regularization parameter is the one which minimizes the function (Golub et al., 1979; Wahba, 1990):

$$V_0(\lambda) = \sum_{k=1}^{N} \{\mathbf{d}_k^{obs} - \mathbf{d}_k^{calc}[\mathbf{m}_k^{est}]\}^2. \qquad (13)$$

This is the conventional cross validation function. The same function can be evaluated in a more efficient way, not demanding for the solution of the inverse problem for each ommited information, by using the following expression (Wahba, 1990):

$$V_0(\lambda) = \sum_{i=1}^{N} \frac{\left[\mathbf{d}_i^{obs} - \mathbf{d}_i(\mathbf{m}_\lambda)\right]^2}{\left[1 - A_{ii}(\lambda)\right]^2}, \qquad (14)$$

where $\mathbf{m}_\lambda = \left(G^T G + \lambda D_l^T D_l\right)^{-1} G^T \mathbf{d}^{obs}$ is the solution of the inverse problem for a particular value of λ, and A_{ii} is the i-th element of the diagonal matrix $A(\lambda) = G\left(G^T G + \lambda D_l^T D_l\right)^{-1} G^T$. The conventional cross validation function is not invariant under an orthogonal transformation of L and $\mathbf{d}^{obs}$. Thus, the value of λ that minimizes V_0 for the transformed problem will not be the same that minimizes V_0 for the original problem, providing different inversion results for two related problems. Modifying the expression of conventional cross validation function on obtains the generalized cross validation function or GCV as given by Wahba (1990):

$$V_0(\lambda) = \frac{\left\|\mathbf{d}^{obs} - \mathbf{d}(\mathbf{m}_\lambda)\right\|^2}{\{\mathrm{trace}[\mathrm{I} - \mathrm{A}(\lambda)]\}^2}, \qquad (15)$$

is invariant under an orthogonal transformation.

For the solution of a non-linear problem one uses an iterative procedure, where GCV can be applied in each step of the linearized inversion. In the last iteration, if there is convergence, the changes in model parameters will be small, being the linearized approximation an adequate description of the problem. Thus on can apply GCV both to linear and non-linear problems, that is, since the estimate of optimum regularization parameter in the first iterations is near the last ones, this approach can be used in non-linear problems. This means that GCV treats in a distinct way the Gaussian noise in observed data in relation to errors generated by the linearized inversion scheme.

IV DIFFRACTION TOMOGRAPHY MODELING VIA BORN APPROXIMATION

The wave equation is given by

$$\nabla^2 U(\mathbf{r}, t) = \frac{1}{c^2(\mathbf{r})} \frac{\partial^2 U(\mathbf{r}, t)}{\partial t^2}, \qquad (16)$$

where $U(\mathbf{r}, t)$ is the solution, either displacement or pressure, and $c(\mathbf{r})$ is the acoustic velocity of the medium. Considering that the solution can be written as $U(\mathbf{r}, \omega, t) = e^{-i\omega t} P(\mathbf{r}, \omega)$, which represents a harmonic dependence with time, we obtain the Helmholtz equation:

$$[\nabla^2 + k^2] P(\mathbf{r}, \omega) = 0, \qquad (17)$$

where the two-dimensional wavenumber is given by $k = k(\mathbf{r}, \omega) = \sqrt{k_x^2 + k_y^2}$. The conditions for the imaging are that the medium is acoustic and 2–D, and the propagation of the incident field is within a limited area $A(\mathbf{r}')$, the background, with constant velocity c_0.

The object function is defined as

$$O(\mathbf{r}) = 1 - \frac{c_0^2}{c^2(\mathbf{r})}, \qquad (18)$$

and represents the perturbation of the velocity in each point in relation to c_0. Redefining the wavenumber as function of $O(\mathbf{r})$, and substituting it in the Helmholtz equation, we obtain

$$[\nabla^2 + k^2] P_S = k_0^2 O(\mathbf{r}) [P_O + P_S], \qquad (19)$$

where P_O is the incident field and P_S is the scattered field. The last differential equation has the following integral solution, known as Lippmann-Schwinger equation (Lo and Inderwiesen, 1994):

$$P_S(\mathbf{r}) = -k_0^2 \int_{A(\mathbf{r}')} O(\mathbf{r}')G(\mathbf{r}|\mathbf{r}')[P_O(\mathbf{r}') + P_S(\mathbf{r}')]d\mathbf{r}'. \tag{20}$$

In the inverse scattering procedure, we consider the knowledge of the scattered field, so that the object function is the unknown function, and the integral solution becomes an integral equation. The above equation is non linear and the linearization is achieved, for example, via the first order Born approximation, which is only valid for the weak scattering of the incident field. The total field is $P_T(\mathbf{r}) = P_O(\mathbf{r}) + P_S(\mathbf{r})$ and $P_S(\mathbf{r}) << P_O(\mathbf{r})$, so that we have $P_T(\mathbf{r}) = P_O(\mathbf{r})$. Thus we obtain a linear relation between $O(\mathbf{r})$ and $P_S(\mathbf{r})$:

$$P_S(\mathbf{r}) = -k_0^2 \int_{A(\mathbf{r}')} O(\mathbf{r}')G(\mathbf{r}|\mathbf{r}')P_O(\mathbf{r}')d\mathbf{r}'. \tag{21}$$

We represent the incident field by a source in $\mathbf{r}_S$ through the Green's function:

$$P_O(\mathbf{r}') = G(\mathbf{r}'|\mathbf{r}_S), \tag{22}$$

and the scattered field in $A(\mathbf{r})$ is registered by a receptor in $\mathbf{r}_G$:

$$P_S(\mathbf{r}_S, \mathbf{r}_G) = -k_0^2 \int_{A(\mathbf{r}')} O(\mathbf{r}')G(\mathbf{r}'|\mathbf{r}_S)G(\mathbf{r}_G|\mathbf{r}')d\mathbf{r}'. \tag{23}$$

The discretization of the above relation leads to the linear relation $\mathbf{d} = A\mathbf{m}$, which has to be inverted in order to recover $O(\mathbf{r})$. In this work the inversion is done using SVD with regularization, which we described earlier.

V NUMERICAL SIMULATIONS

We explore the GCV approach for the selection of the regularization parameter in four synthetic examples, all with 225 blocks (15 × 15), that is, the vector of model parameters has 225 components. In all numerical experiments there are 16 sources and 16 receivers, in such a way that the data set has 256 complex numbers. Since we separate the complex numbers in real and imaginary parts, we have in fact 512 informations, making the tomographic matrix overdetermined (512 equations × 225 unknowns). The frequency of the monochromatic wave is 200 Hz, and all the simulations were performed with noisy data. Basically we added Gaussian noise in such a level that the RMS error between the original scattered field and the corrupted one is around 1 %. For each example and for each order, we produced three GCV curves. Due to space limitations we display only some results, although all simulations are summarized in Table I, where the estimator ϵ^c_{rms} express the rms error of the acoustic velocity:

$$\epsilon^c_{rms} = \frac{\sqrt{\sum_{i=1}^{N}(c_i^{true} - c_i^{est})^2}}{\sqrt{\sum_{i=1}^{N}(c_i^{true})^2}} \times 100\ \%. \tag{24}$$

In the Table I, besides the results with GCV we also provide the results from L-curve and Θ-curve, taken from Santos and Bassrei (2007).

The scattered field was computed using a second order in time and fourth order in space, finite differences scheme. We adopted a Ricker's wavelet centered around 200 Hz as source, propagating through the medium limited by absorbing boundaries. The calculation of the scattered field can be separated in two steps: first we compute the primary field assuming an homogeneous medium with background velocity. Then we use the velocity model to compute the total field. We obtain the scattered field subtracting the primary field from the total field. The resulting scattered field was deconvolved at 200 Hz as center frequency in order to perform a monochromatic inversion. The calculated field at the source position has some differences of amplitude and phase in relation to the original Ricker's wavelet due to the modeling, which were adjusted using an average complex correction factor.

The first synthetic example simulates the diffractor point. The background medium has 4,000 m/s, and the inhomogeneity (diffractor point) is represented by a single block with 4,100 m/s, which means a 2.5 % positive anomaly. Figure 1 shows the true model. The diffractor point is in fact a 10 m × 10 m square or half wavelength × half wavelength. Figure 2 shows the GCV curve for zero order, and its minimum value was used to obtain the estimated model, showed in Figure 3. For the second order, the GCV curve, and the reconstructed model, are respectively, showed in Figures 4 and 5. The non-regularized solution, using standard least squares, is showed in Figure 6. We notice that the three GCV curves are very similar (the first order is not showed here), and consequently, the results for zero, first, and second orders regularizations are also very similar. This can also be seen by checking Table I. For this example the regularized solution was not better that the non-regularized least squares.

In the second example there is an homogeneous inclusion in the form of a plus pod within the homogeneous background, which has 3,000 m/s. The inclusion (plus pod) has 3,300 m/s, which represents a positive anomaly of 10 %. The plus pod true model can be seen in the Figure 7. In terms of wavelength, the plus pod has a diameter of 5.3 wavelengths. Figure 8 shows the GCV curve for zero order. The minimum value of Figure 8 was used to obtain the estimated model showed in Figure 9. For the second order the GCV curve, and the reconstructed model, are respectively, showed in Figures 10 and 11. The least squares solution is presented in Figure 12. Comparing Figure 12 to Figure 09 or to Figure

11, we can conclude the necessity of some kind of regularization. The results displayed in Table I corroborate this conclusion.

The third example, displayed in Figure 13, is a simple representation of a reef, as a possible oil reservoir. The acquisition geometry is still the cross-hole, like the first and the second examples. The background medium has 4,000 m/s. There is also a low velocity layer, with 3,900 m/s, which means a minus 2.5 % contrast. The central inhomogeneity (the reef) has 4,100 m/s which is equivalent to a plus 2.5 % anomaly. In terms of wavelength the reef is 3.5 wavelengths $\times$ 1 wavelength, and the low velocity layer is 7.5 wavelengths $\times$ 1 wavelength. Figure 14 shows the GCV curve for zero order. The minimum value of Figure 14 was used to obtain the estimated model showed in Figure 15. For the second order the GCV curve, and the reconstructed model, are respectively, showed in Figures 16 and 17. The least squares solution is presented in Figure 18. Figure 18 displays a reasonable result, but if compared to the regularized solutions, that is, Figure 15 or Figure 17, it is the worst image, and with the highest value of the ϵ^c_{rms} estimator. The best result, both in terms of quality and quantity, is provided by the second order regularization.

For the VSP geometry, the true model is the same showed in Figure 13. The sources are still located in a hole but the receivers are now located at the surface. Figure 19 shows the GCV curve for zero order, and its minimum was used to obtain the estimated model showed in Figure 20. For the second order the GCV curve, and the reconstructed model, are respectively, showed in Figures 21 and 22. The least squares solution is presented in Figure 23, which is completely inconsistent. The image obtained with zero order regularization is also very poor, and the first order (not showed) is poor to reasonable, whereas the second order provided the best image. Again, the results displayed in Table I corroborate this conclusion.

VI CONCLUSIONS

From four sets of overdetermined synthetic examples corrupted by noise and with an ill-conditioned kernel matrix we have shown that the regularization algorithm in question, together with the use of GCV for the selection of the regularization parameter, is feasible in linear geophysical diffraction tomography. The two last sets represent the same simple geological model but with different acquisition geometries, cross-hole and VSP, this last one very common in geophysical exploration for hydrocarbon reservoirs. The comparison with non-regularized solution confirms the necessity of some kind of regularization. We considered three orders of regularization, where the order of regularization is equivalent to the order of the derivative matrix. One crucial aspect here is the selection of regularization parameter, usually chosen by some trial and error approach. The results with GCV were consistent, providing good to excellent approximations of the true model, even considering that Gaussian noise was always added to the scattered field, and the observed data was not exact, that is, it did not came from the first order Born series, but from a finite differences scheme. In general GCV proved to be more efficient than the other two approaches, used for comparison: L-curve and Θ-curve. Natural extensions of this work are the application of this formulation to a layered medium background, and to real data waveform.

REFERENCES

Bassrei, A., and Rodi, W. L., (**1993**). "Regularization and inversion of linear geophysical data". In: 3rd International Congress of the Brazilian Geophysical Society, Rio de Janeiro, Brazil, vol. 1, pp. 111–116.

Devaney, A. J., (**1984**). "Geophysical diffraction tomography," IEEE Transactions on Geoscience and Remote Sensing **22**, 3–13.

Farquharson, C. G., and Oldenburg, D. W., (**2004**). "A comparison of automatic techniques for estimating the regularization parameter in non-linear inverse problems," Geophysical Journal International **156**, 411–425.

Golub, G., Heath, M., and Wahba, G., (**1979**), "Generalized cross validation as a method for choosing a good ridge parameter," Technometrics **21**, 215–224.

Lo, T.-w., and Inderwiesen, P. L., (**1994**). *Fundamentals of Seismic Tomography* (Society of Exploration Geophysicists, Tulsa, OK)

Reiter, T. D., and Rodi, W., (**1996**). "Nonlinear waveform tomography applied to crosshole seismic data," Geophysics **61**, 902–913.

Rocha Filho, A. A., Harris, J. M., and Bassrei, A., (**1996**). "A simple matrix formulation diffraction tomography algorithm." In: 39th Brazilian Congress of Geology, Salvador, Brazil, vol. 2, pp. 312–315.

Rocha Filho, A. A., Harris, J. M., and Bassrei, A., (**1997**). "Integrated inversion of seismic data using diffraction tomography (in Portuguese)." In: 5th International Congress of the Brazilian Geophysical Society, São Paulo, Brazil, vol. 2, pp. 630–634.

Santos, E. T. F., and Bassrei, A., (**2007**). "L- and Θ-curve approaches for the selection of regularization parameter in geophysical diffraction tomography," Computers & Geosciences **33**, 618–629.

Slaney, M., Kak, A. C., and Larsen, L. E., (**1984**). "Limitation of Imaging with First-order diffraction Tomography," IEEE Transactions on Microwave Theory and Techniques **32**, 860–874.

Thompson, D. R., Rodi, W., and Toksöz, M., N., (**1994**), "Nonlinear seismic diffraction tomography using minimum structure constraints," Journal of the Acoustical Society of America **95**, 324–330.

Titterington, D.M., (**1985**), "General structure of regularization procedures in image reconstruction," Astronomy and Astrophysics **144**, 381–387.

Twomey, S., (**1963**), "On the numerical solution of Fredholm integral equations of the first kind by the inversion of the linear system produced by quadrature," Journal of the Association of Computing Machines **10**, 97–101.

Wahba, G., (**1990**), *Splines models for observational data* (Society for Applied and Industrial Mathematics, Philadelphia)

Wu, R-S, and Toksöz, M. N., (**1987**), "Diffraction tomography and multisource holography applied to seismic imaging," Geophysics **52**, 11–25.

Yao, Z. S., and Roberts, R. G., (**1999**), "A practical regularization for seismic tomography," Geophysical Journal International **138**, 293–299.

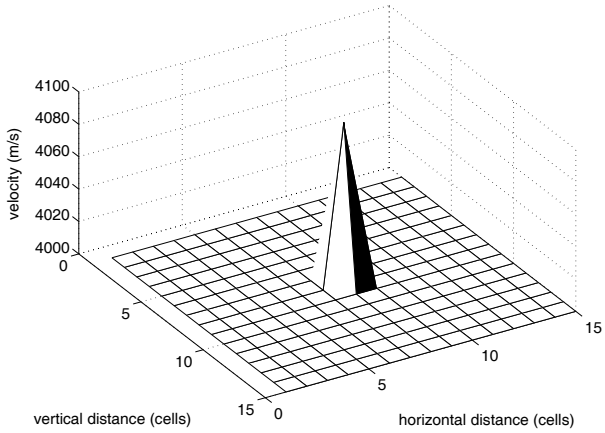

FIG. 1. Example 1. Diffractor point model. 3-D representation of the true model.

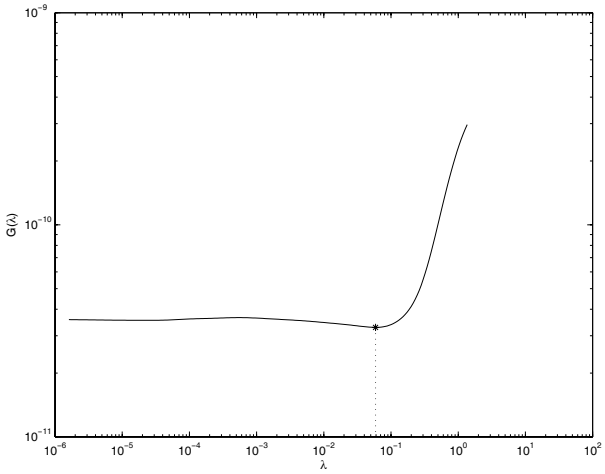

FIG. 2. Example 1. Diffractor point model. GCV curve for zero order.

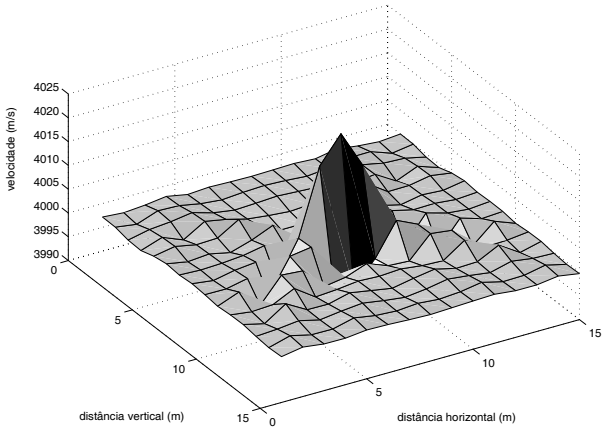

FIG. 3. Example 1. Diffractor point model. Estimated tomogram for zero order.

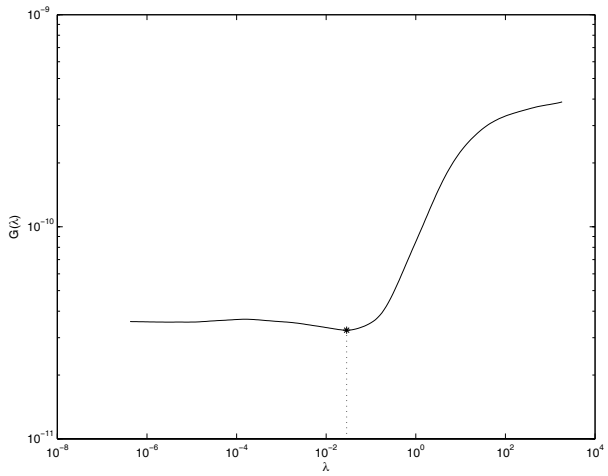

FIG. 4. Example 1. Diffractor point model. GCV curve for second order.

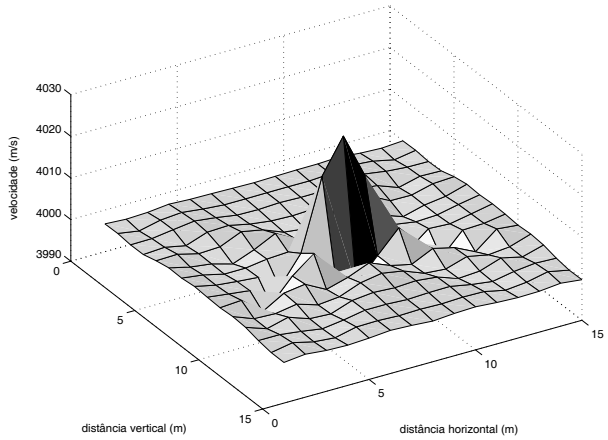

FIG. 5. Example 1. Diffractor point model. Estimated tomogram for second order.

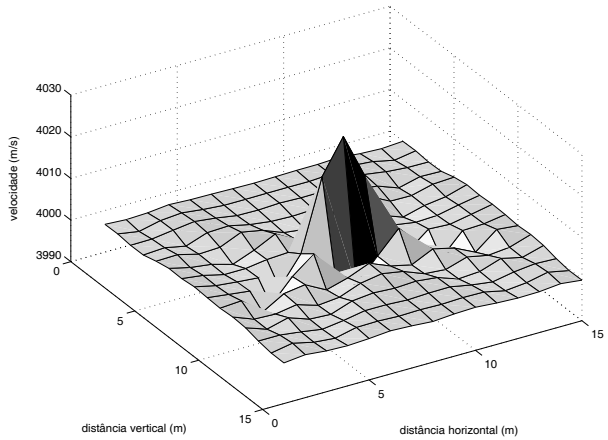

FIG. 6. Example 1. Diffractor point model. Estimated tomogram using least squares.

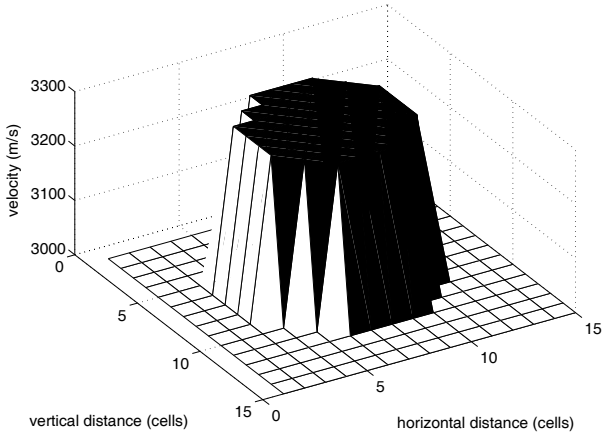

FIG. 7. Example 2. Plus pod model. 3-D representation of the true model.

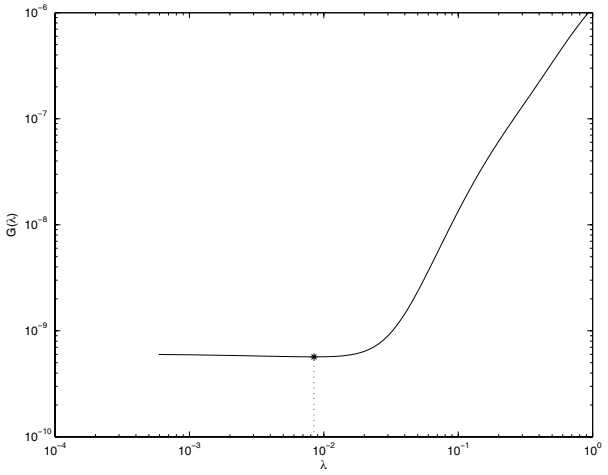

FIG. 8. Example 2. Plus pod model. GCV curve for zero order.

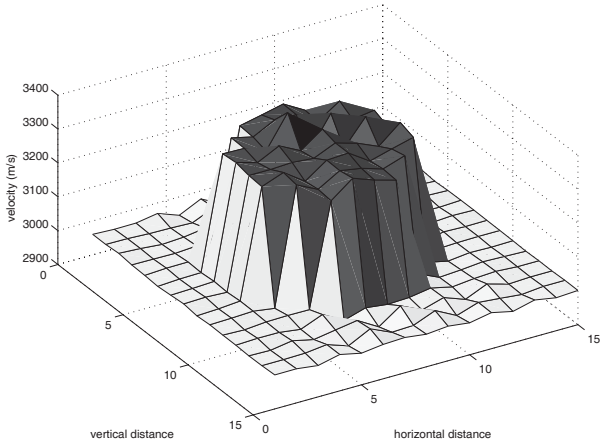

FIG. 9. Example 2. Plus pod model. Estimated tomogram for zero order.

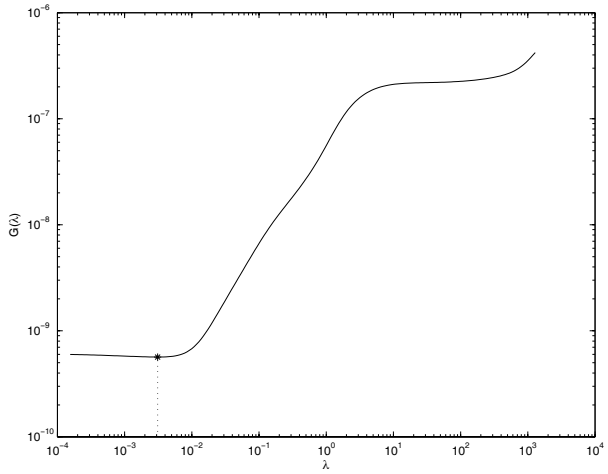

FIG. 10. Example 2. Plus pod model. GCV curve for second order.

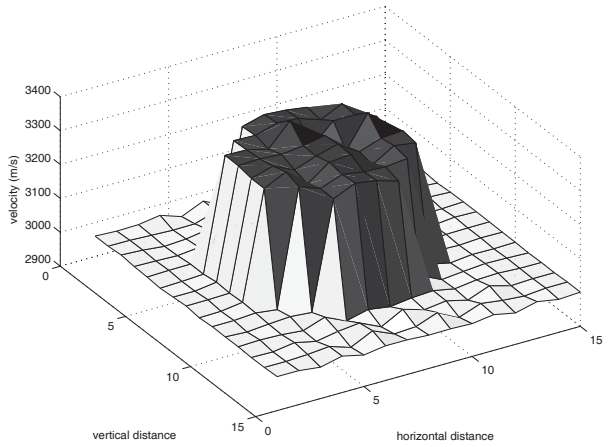

FIG. 11. Example 2. Plus pod model. Estimated tomogram for zero order.

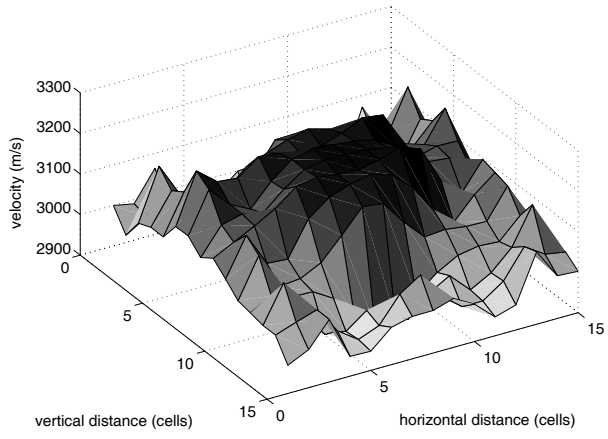

FIG. 12. Example 2. Plus pod model. Estimated tomogram using least squares.

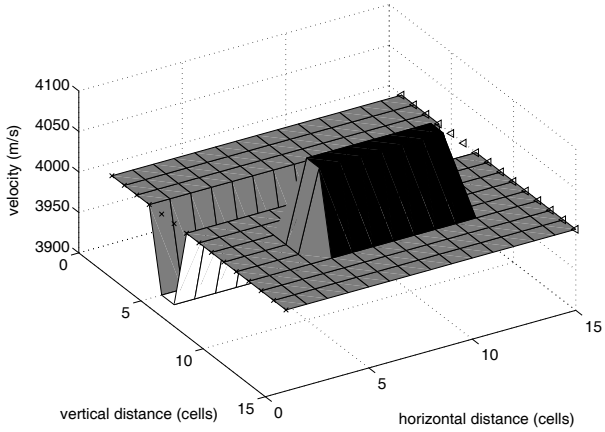

FIG. 13. Example 3. Simple reef model. Cross-hole and VSP geometries data acquisition. 3-D representation of the true model.

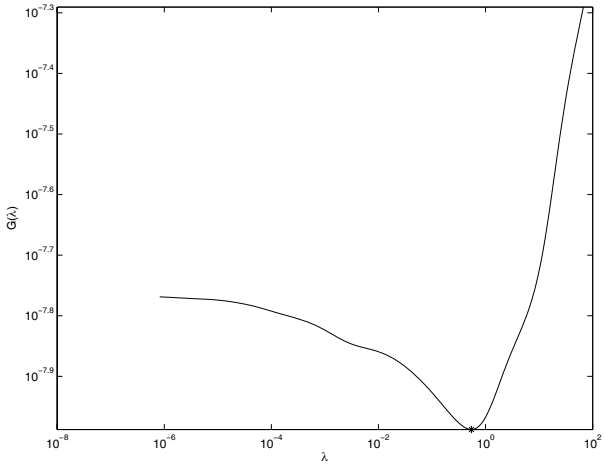

FIG. 14. Example 3. Simple reef model. Cross-hole geometry data acquisition. GCV curve for zero order.

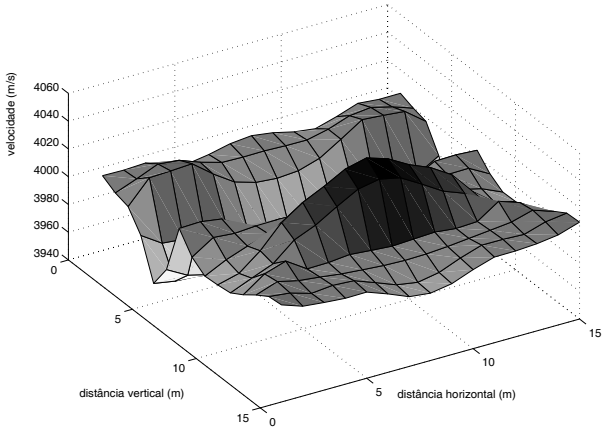

FIG. 15. Example 3. Simple reef model. Cross-hole geometry data acquisition. Estimated tomogram for zero order.

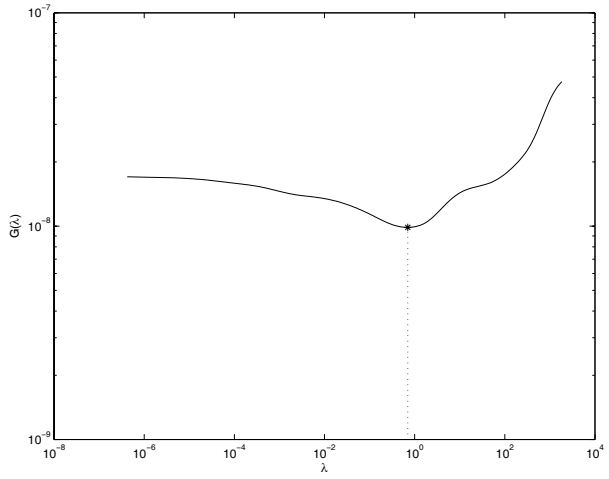

FIG. 16. Example 3. Simple reef model. Cross-hole geometry data acquisition. GCV curve for second order.

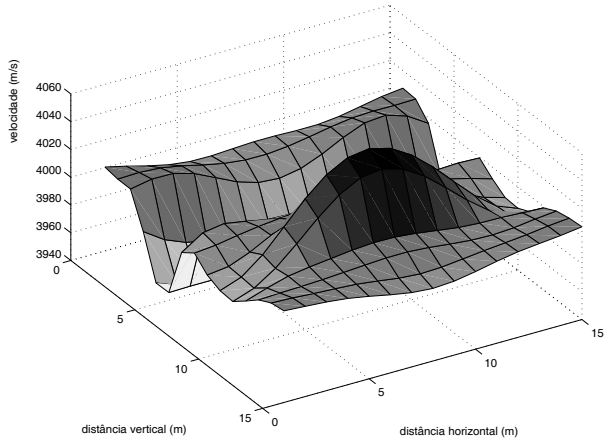

FIG. 17. Example 3. Simple reef model. Cross-hole geometry data acquisition. Estimated tomogram for second order.

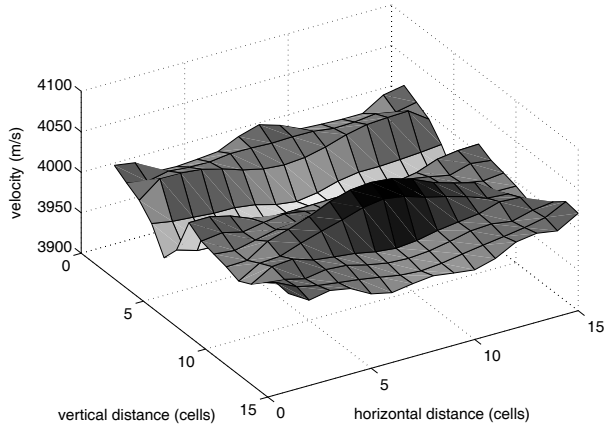

FIG. 18. Example 3. Simple reef model. Cross-hole geometry data acquisition. Estimated tomogram using least squares.

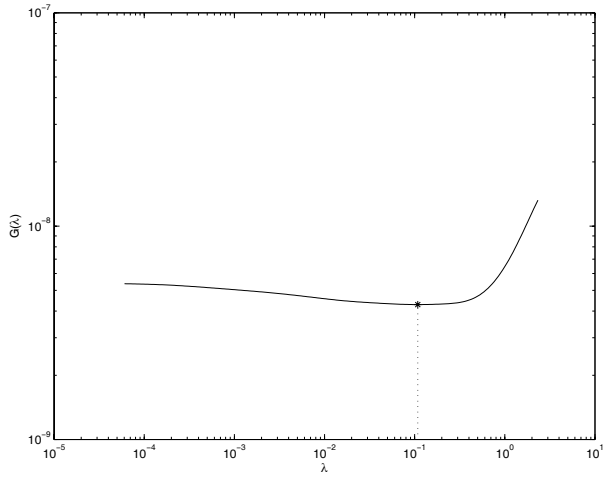

FIG. 19. Example 4. Simple reef model. VSP geometry data acquisition. GCV curve for zero order.

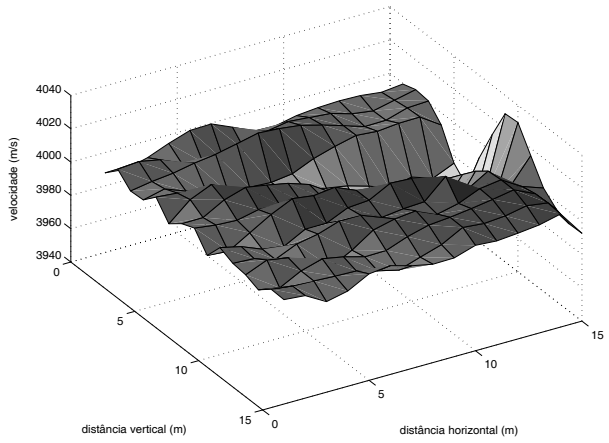

FIG. 20. Example 4. Simple reef model. VSP geometry data acquisition. Estimated tomogram for zero order.

Acknowledgments

This work is part of the project "Velocity inversion in traveltime tomography and macro-model determination for seismic migration" (edict MCT/CNPq 02/2006 - Universal).

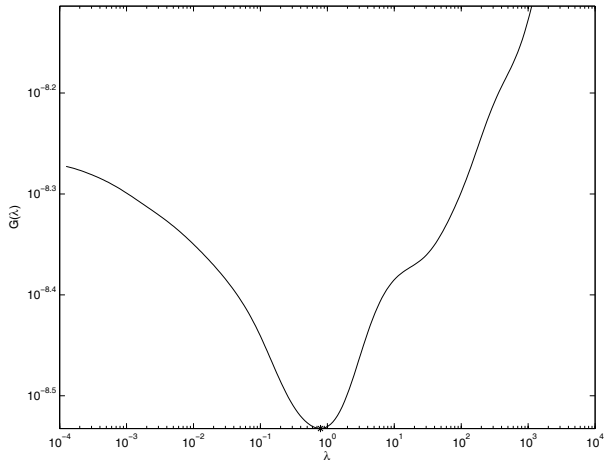

FIG. 21. Example 4. Simple reef model. VSP geometry data acquisition. GCV curve for second order.

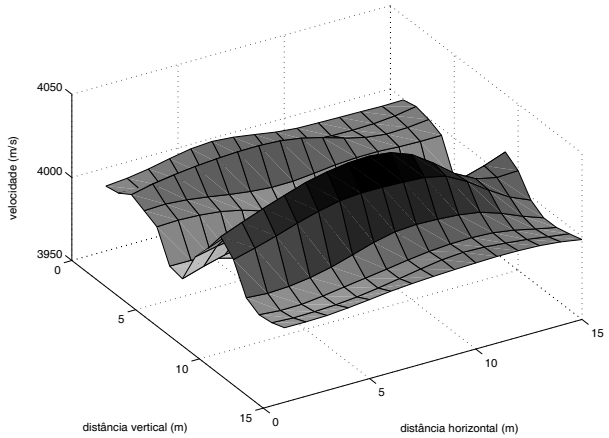

FIG. 22. Example 4. Simple reef model. VSP geometry data acquisition. Estimated tomogram for second order.

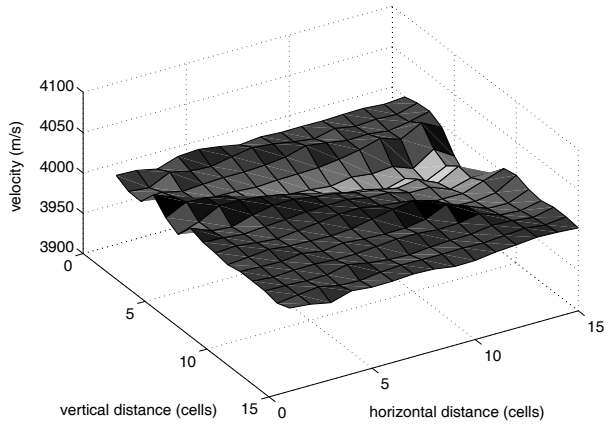

FIG. 23. Example 4. Simple reef model. VSP geometry data acquisition. Estimated tomogram using least squares.

model	method	λ_{best}	ϵ^c_{rms} (%)
	order 0: L-curve	0.0008	0.07
	order 0: Θ-curve	0.0666	0.06
example 1	order 0: GCV	0.0589	0.06
	order 1: L-curve	0.0006	0.07
diffractor point	order 1: Θ-curve	0.0769	0.05
	order 1: GCV	0.0435	0.06
cross-hole	order 2: L-curve	0.0003	0.07
	order 2: Θ-curve	0.0514	0.05
	order 2: GCV	0.0286	0.06
	least squares	—	0.06
	order 0: L-curve	0.0060	0.69
	order 0: Θ-curve	0.0045	0.78
example 2	order 0: GCV	0.0084	0.60
	order 1: L-curve	0.0111	0.52
plus pod	order 1: Θ-curve	0.0061	0.55
	order 1: GCV	0.0058	0.56
cross-hole	order 2: L-curve	0.0041	0.53
	order 2: Θ-curve	0.0038	0.54
	order 2: GCV	0.0031	0.56
	least squares	—	2.68
	order 0: L-curve	0.1234	0.51
	order 0: Θ-curve	0.1322	0.51
example 3	order 0: GCV	0.2100	0.50
	order 1: L-curve	0.1599	0.51
reef	order 1: Θ-curve	0.3035	0.48
	order 1: GCV	0.5457	0.48
cross-hole	order 2: L-curve	0.2449	0.53
	order 2: Θ-curve	0.4784	0.49
	order 2: GCV	0.7023	0.48
	least squares	—	0.53
	order 0: L-curve	0.2139	0.60
	order 0: Θ-curve	0.2256	0.60
example 4	order 0: GCV	0.1083	0.63
	order 1: L-curve	0.2783	0.55
reef	order 1: Θ-curve	0.2971	0.55
	order 1: GCV	0.6596	0.53
VSP	order 2: L-curve	0.8463	0.53
	order 2: Θ-curve	0.5867	0.54
	order 2: GCV	0.7890	0.53
	least squares	—	0.61

TABLE I. λ_{best} and ϵ^C_{rms} of all simulations.